pH Sensitive Thread-Based Wound Dressing with Integrated Drug Delivery and Wireless Bluetooth Interface

by

Lucas Karperien
BEng, University of Victoria, 2017

A Thesis Submitted in Partial Fulfillment
of the Requirements for the Degree of

MASTER OF APPLIED SCIENCE

in the Department of Mechanical Engineering

Supervisory Committee

pH Sensitive Thread-Based Wound Dressing with Integrated Drug Delivery and Wireless Bluetooth Interface

by

Lucas Karperien

BEng, University of Victoria, 2017

Supervisory Committee

Dr. Mohsen Akbari, Mechanical Engineering
Supervisor

Dr. Caterina Valeo, Mechanical Engineering
Departmental Member

Abstract

Wound treatment is a significant field in healthcare, but one with huge potential and need for advancement. Infection monitoring, in its current state, is a largely primitive affair, relying on visual and olfactory inspection to detect bacteria. As a result, early detection is impossible, and doctors and patients are forced to remove dressings to investigate the wound in a laborious, painful, and unsanitary process. When an infection is detected, the treatment is typically systemic administration of antibiotics. Systemic administration reduces the concentration of antibiotics that can be brought to bear on the infection because it interacts with the entire body and is dissipated by the time it reaches the wound and increases the risk of side effects or antibiotic resistance. Within this thesis, a smart, thread-based wound dressing is presented that addresses these issues by providing a pH-based early detection system accompanied by a topical, on-demand drug delivery system. The device has been tested in vitro and in vivo, on bacterial culture and on an animal model, and demonstrated effectiveness at detecting and eliminating bacteria, and at promoting wound healing. This smart wound dressing has the potential to improve treatment and outcomes for a wide variety of injuries, varying from burns to chronic wounds.

Table of Contents

List of Figures

Acknowledgments

I would like to thank the entire LiME Lab for their help and support, both scientific and emotional. I am especially grateful to Hossein Dabiri for his invaluable assistance, especially in the process of developing and testing the microparticles and throughout the project generally. I think you shed almost as much blood sweat and tears as I did.

And to Zhina Hadisi for her time and expertise on the bacterial and animal work, your contribution has been invaluable.

And David Hamdi for help with electronics questions and being a general sound board for questions and ideas, I hope you don't think I'm completely insane.

I would finally like to thank my supervisor Dr. Akbari for his enthusiasm, encouragement and assistance in this project and for mentoring me in his lab for so long. I've appreciated every minute of my time here, from undergrad to now, and I value the skills and lessons I've learned working with you and the lab.

Dedication

I would like to dedicate this thesis to my parents Wayne and Audrey-Lynn Karperien. Your encouragement of learning, building, inquisitiveness, and science were foundational to my decision to pursue engineering and post-grad education, and your help and encouragement have been vital to me.

Chapter 1: Introduction

1.1 Wounds and Infections

As medical technology in general has advanced, wound monitoring has remained essentially stagnant in methods and technology, overwhelmingly relying on olfactory and visual queues to detect infection [1]. Because visual and olfactory sensing require access to the wound, the wound dressing must be removed in a process that is painful, laborious, and increases the risk of introducing pathogens to the wound. Since infection detection largely depends on symptoms and signs of a well developed infection, early detection and action is virtually impossible [2],[3]. Unsurprisingly, wound infection remains a serious concern. In fact, according to one 2013 study by the Canadian Institute for Health Research, 10% of long-term care patients reported infected wounds [4]. Wound healing is affected in diverse ways by bacterial colonization, falling on a spectrum from potentially beneficial to harmful. Every wound is contaminated with bacteria from the surrounding skin or environment, but if the concentration of pathogenic bacteria grows too large, it begins to have a deleterious effect on wound healing, delaying or even stalling it indefinitely by disrupting cellular cascades and causing biochemical imbalance. As a result, early detection and treatment of pathogenic bacteria is important for wound healing [5].

1.2 Infection Detection

More advanced techniques such as wound swabbing do exist, and serve a purpose for identification of an infection, but are of dubious usefulness for infection detection [6], and thus, clinical analysis of characteristics and symptoms remains the most common technique for initial infection detection [7]. However, there are other potential methods of infection

monitoring, using electrical or chemical methods to provide more effective therapy [8]–[10]. One common technique is pH monitoring, which works because, while human skin is naturally acidic, with a healthy pH between 4 and 6, wound tissue has a pH around 7.4 due to exposure of the internal body fluids [11]. Bacterial colonization will either increase or decrease the pH of a wound depending on the type of bacteria present [12]. pH does vary with temperature, such that the neutral point varies from 7 at 25 ºC to 6.63 at 50 ºC and 7.47 at 0 ºC. This effect becomes more pronounced for strong bases, and less pronounced for strong acids [13]. However, this effect will have negligible impact on the device described herein since the wound bed temperature typically varies only between 31-34 ºC [14], intentional heating will occur only in short bursts, and the relation used to convert between measured pH and infection is determined empirically within the relevant temperature range.

Systemic antibiotic administration is the typical approach for infection treatment, but there are several advantages to topical administration, which is the alternative. Topical antibiotics can be administered with greater control, in higher doses, and without the same concern for side effects or developing resistance [10], [15].

1.3 Previous Art

An emerging field of healthcare technology is smart dressings, which are wound dressings that respond to the chemical and biological conditions of the wound area [16]. These smart dressings can be used for diagnostics, treatment or both. Medical textiles are another developing market with a high potential for growth and change in the medical field, involving anything from gauze to sutures [17]. Miniaturizing technology allows for the

development of wearable devices, or smart dressings that can be used as point-of-care diagnostics for wound monitoring in hospital and home settings [16].

1.3.1 Colorimetric

Colorimetric sensing is one method of wound monitoring used in smart dressings, where colour changes in response to biomarkers such as pH are analyzed optically to determine the state of the wound bed. An example of such a smart dressing is a work by Mirani et al, which uses colour changing pH sensitive patches in a hydrogel wound dressing to monitor for infection using a smartphone interface [10]. In this work, alginate-suspended colour-changing beads were 3D printed to form pH sensitive lattices in a flexible hydrogel bandage. The hydrogel bandage structure is both flexible and effectively provides a moist environment to promote wound healing. The pH sensitive patches are loaded with Brilliant Yellow—a dye that changes colour according to the pH of its environment—and are imaged by a cell-phone app which is able to determine the pH from the colour compared to a reference. The dressing also contains drug eluting scaffolds, loaded with gentamicin sulfate.

Another work by Koh et al. presents a microfluidic-based colorimetric sweat monitor. This device is not, strictly speaking, a wound dressing, but it is a flexible, skin-mounted, colorimetric device, used to monitor sweat loss, pH, sweat glucose (which is correlated with blood glucose), and other biomarkers [18]. This device uses a cell phone app to interpret colorimetric data, and localized chemical analyses that respond to different ions or biomarkers, providing a complex map of information regarding the chemical composition of sweat. The microfluidics channels uptake and guide the sweat into

channels, where it is stored and reacted with analytes, and then imaged for analysis. In addition, flexible electronics embedded in the device provide wireless data on skin temperature. Other works similarly monitor sweat using colorimetric methods [19],[20],[21].

A 2017 work by Kassal et al. describes a colorimetric wound-monitoring device that relies on an integrated optoelectronic device for colour interpretation rather than a smart phone camera [22]. This device uses an LED and a photodiode to measure the colour of a pH indicator die, GJM-534, covalently bonded to cellulose particles and encapsulated in a film of Hydromed D4, a polyurethane based hydrogel. The bandage transmits data from the photodiode to a cell phone for analysis.

These colorimetric approaches are limited by their low precision and the need for transparent substrates that makes them difficult to use in cases where the wound is covered in a non-transparent dressing, such as burn wounds.

1.3.2 Electrochemical

There are also a number of works developing electrochemical sensors, which use chemical reactions with biomarkers to modify electronic signals, measuring the response and transmitting the data wirelessly to a receiver. However, they lack the flexibility, ease of integration with existing technology, and closed-loop drug delivery systems that could make them truly effective and autonomous smart wound dressings. These devices, such as the one developed by Kassal et al [23], can be much more precise than colorimetric ones and require less user-input. The dressing made by Kassal et al. uses an enzymatic reaction to produce hydrogen peroxide by reaction with uric acid, and a potentiostat to reduce it and

produce a measurable current. Uric acid is an indicator produced in wounds that indicates both healing and infection, making it a powerful marker to analyze. The device was made by screen printing carbon and silver inks on a regular bandage, with a specially designed potentiostat providing square wave voltammetry and wireless communications.

Another work by Mostafalu et al. details the development of a screen printed oxygen-sensitive smart bandage [24]. Oxygen level is another indicator for healing in chronic wounds. The device is designed to be flexible and wireless, using flexible electronics to make a sensor using zinc and carbon electrodes on a parylene substrate, and a galvanic hydrogel to produce a current proportional to the oxygen level.

A different work by Mostafalu et al. uses pH sensors to monitor a wound, and delivers antibiotics using thermoresponsive microparticles [9]. In this device, carbon and polyaniline (PANI) electrodes serve as working electrodes in a potentiometric reaction with pH, producing a voltage drop against the silver reference electrode. The electrodes are screen printed on polyethylene terephthalate, PET, a flexible polymer film, and monitor the pH of the wound bed to detect infection. In addition, a parallel system comprising a gold heating element and thermoresponsive microspheres loaded with antibiotics and suspended in a hydrogel exists to eliminate any infection that is detected. This system is very similar to the one developed here, using the same principles of drug-delivering thermoresponsive microspheres and PANI-based electrochemical pH monitoring, but in a screen-printed rather than thread-based substrate.

Thread-based pH sensors for wound monitoring have been demonstrated in another work by Punjiya et al. [25], using PANI electrochemical pH monitoring in a wireless smart

dressing. A separate work by Mostafalu et al. presents silver coated threads as heating elements for drug delivery with thermoresponsive microparticles [26]. These works demonstrate the previously mentioned effectiveness of threads as substrates for functionalization [27], as they are flexible, versatile and easily mass produced. The work done in this thesis is built on previous work done on thread-based sensors, and integrates the diverse systems into a unified, closed-loop system for wound monitoring and treatment. Flexible pH sensitive and drug releasing threads are combined in a system that monitors wounds for infection, and delivers topical antibiotics on demand, all while remaining versatile enough to be incorporated with existing dressings such as gauze in burn wounds.

1.4 Device Design

This thesis presents the development of a thread-based smart wound dressing, using pH sensitive elements to detect infection and deliver topical antibiotics on demand. A schematic is shown below in Figure 1,with the basic design of the patch and smart phone interface. In this design, the pH of the wound bed is monitored with functionalized threads connected to an Arduino. pH monitoring threads use polyaniline (PANI), a pH sensitive polymer, to form an electrochemical pH sensor. The condition of the wound is assessed, and relevant data sent to the user's phone via Bluetooth. If bacterial infection is detected, heating is triggered into a heating element, releasing the antibiotics. This sensor system, being thread based, is flexible and versatile and an easily be incorporated under or sewn into a standard wound dressing and can be used in burn wounds and chronic wounds. The wireless interface and built-in control system make it user friendly and effective for hospital and home use.

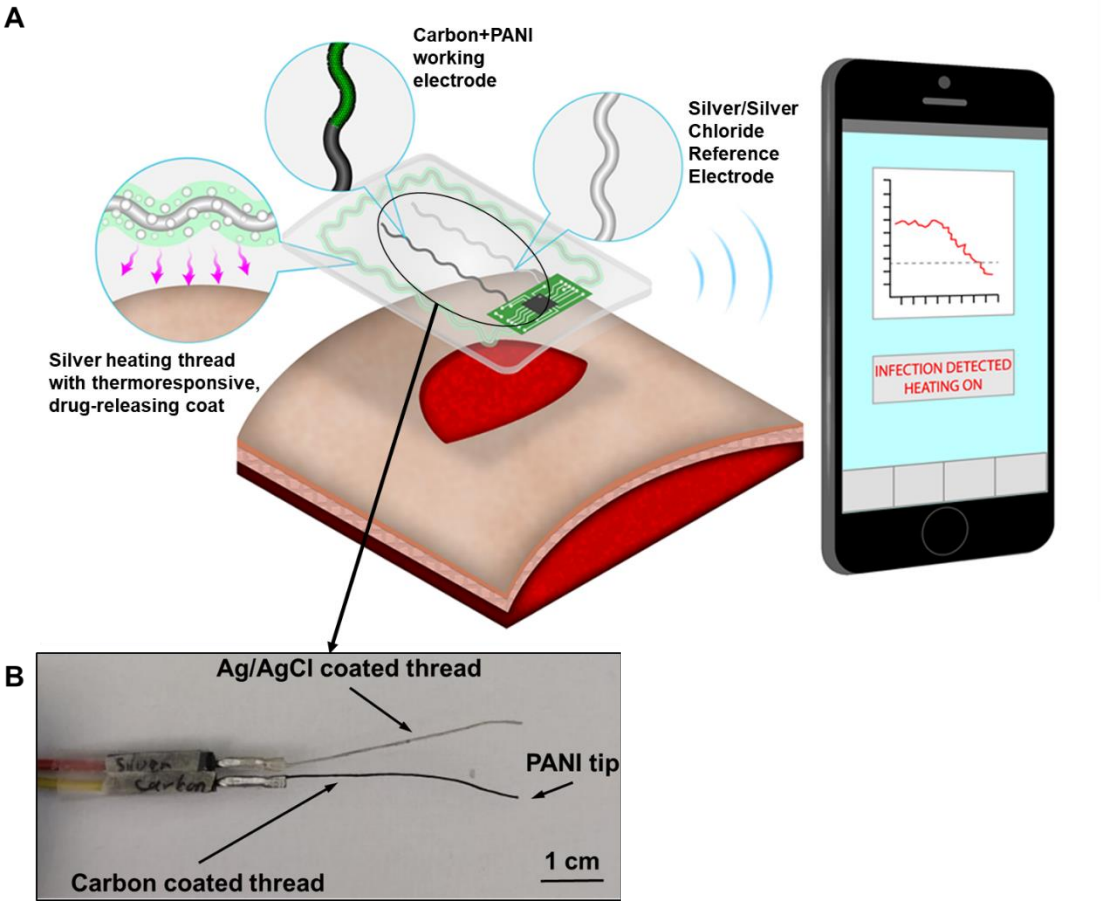

Figure 1: A) Schematic showing the concept of the smart bandage. pH sensors monitor the wound site and interface with a Bluetooth chip transmitting to a cell phone, while drug releasing threads are ready to administer antibiotics as needed. B) Photograph of the pH sensitive threads.

Chapter 2: Thread Functionalization and Characterization

2.1 Coating

The base materials of this project are functionalized threads. Humble cotton threads coated and modified with inks, polymers, and hydrogels to perform a variety of tasks from biosensing to heating. As such a foundational and significant portion of the project, this topic is deserving of its own chapter.

2.1.1 Conductive Threads Background

The basic concept of medical textiles, textile engineering, and functionalized threads is by no means unique or novel to this project. Mostafalu et al. have published a significant work detailing a variety of functionalized thread types and applications, including pH and strain sensors [27]. While many different substrates can be used to produce the same kind of devices [9], [10], thread-based technology has unique advantages in that it is easily mass produced and is extremely versatile. Threads can be sewn, woven, braided or otherwise manipulated in many ways to produce the desired configuration for any particular device [28], [29]. Medical textiles in general are a growing field, as doctors and researchers look to progress beyond the basic gauze and sutures that make up the bulk of medical textiles [17].

2.1.2 Inks and Polymers

A number of different kinds of threads were produced for this project and required different kinds of coatings, each providing unique challenges.

2.1.2.1 Ink Coating device

One of the primary materials used for functionalizing threads was conductive ink, provided by Engineered Conductive Materials (100 Innovation Ct. Delaware, OH, USA), a branch of Engineered Material Systems, Inc. All of the functionalized threads used in this project were first treated with an Enercon Industries Corporation Dyna-A-Mite 3D treater to improve adhesion, then functionalized with conductive ink before moving on to more advanced polymer or hydrogel coats. The working and reference electrodes of the pH sensor are made from carbon and silver/silver chloride coated threads respectively, while the drug releasing elements are made from silver coated threads. Accordingly, the ability to reliably and consistently coat threads was a primary challenge to address. The inks used were too viscous for simple dip coating, as they would form thick, un-controlled agglomerations on the thread rather than an even coat. Finger coating, smoothing the ink down into a thin layer by passing the thread between gloved fingers, was a useful primary technique for proof of concept work, but yielded inconsistent and unscientific results. As a result, a device was developed, shown below in Figure 2, to create more even and uniform coats. The device consists of a capsule containing the desired conductive ink (silver, silver/silver chloride, or carbon) with a PDMS plug. The thread is passed through a hole in the PDMS such that it forms a seal around the thread, acting as a squeegee as the thread is drawn through it. The effectiveness of the device was tested by comparing the relative standard deviation (RSD) of resistance on threads coated with carbon ink using the device and using finger coating. RSD is defined as the standard deviation divided by the mean, as shown below.

$$RSD = \frac{standard\ deviation}{mean} \quad (1)$$

Both the inter-thread RSD, showing the variation between threads, and the intra-thread RSD, showing the variation within an individual thread, were compared. They were measured using a multimeter with triplicate biological replicate samples, three samples per condition. In both cases the extrusion coater was superior to the hand coating technique, producing more even coats on individual threads and more even threads.

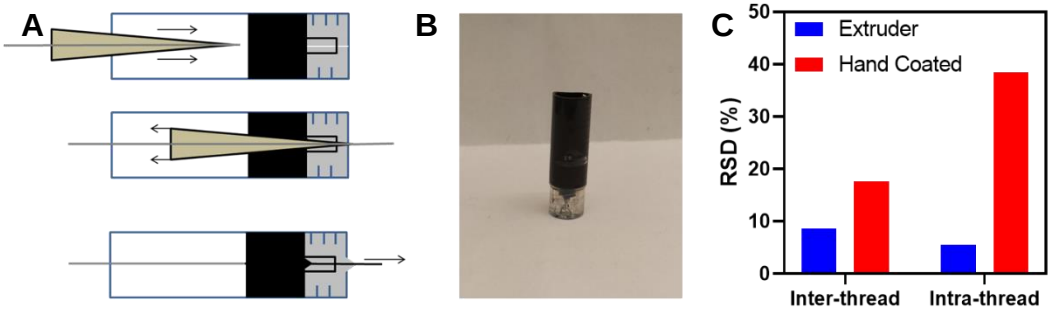

Figure 2: A) Extrusion coater schematic, showing the basic operation. A thread is passed through the ink well and PDMS channel using a pipette tip as an insertion device, then the pipette tip is withdrawn, and the thread is passed through the rest of the way. B) Photograph of the device C) Comparison of the RSD of the extrusion coater to hand-coating techniques. Inter-thread RSD shows variation between different threads, while intra-thread RSD shows the consistency of the coat within the individual threads.

It was found that the conductivity of the threads increased with more layers, as did the consistency both within and between threads, as shown below in Figure 3. Inter-thread consistency is important because variation in resistance between samples introduces a source of error to experiments, and the RSD of resistance between threads was lowest after 3 coats, reaching a minimum value of 8.7%. Adding further coats after this point slowly

increased the RSD, likely because the size of the hole in the extruder was limiting it's coating ability. The intra-thread RSD, representing the evenness of the coat on an individual thread, is also significant, especially for heating elements, where concentrations of resistance will lead to uneven heating. This value was found also to be lowest at about 3 coats, with a value of about 5.5 %.

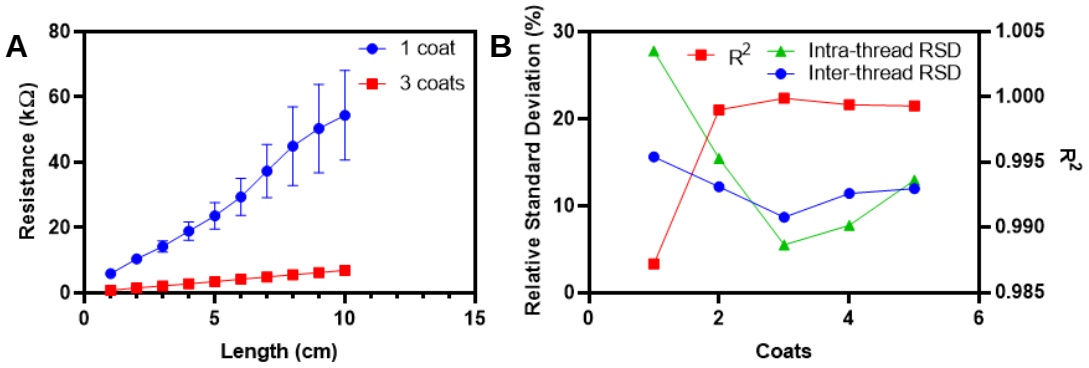

Figure 3: A) Resistance per cm for carbon ink coated threads at 1 and 3 coats, showing that resistivity varies wildly after one coat, but becomes extremely consistent after 3. Error bars indicate standard deviation, calculated from samples in triplicate. B) Relative Standard Deviation values for 10 cm threads, showing that consistency peaks at about 3 coats, while linearity (R^2) remains approximately the same after 2.

2.1.2.2 Dip Coating PANI

Polyaniline (PANI), is a polymer that undergoes conformational change in the presence of hydronium ions, reaching an equilibrium state and creating a voltage with a slightly super-Nernstian response [30]. This electrochemical pH sensitivity is the basis of the pH sensors developed in this project. In order to produce the threads, the PANI was dissolved in 0.1 M HCl solution at 4 ^{0}C for 24 hours, and the carbon coated threads dipped in the solution for one minute while gently agitating the solution, then left to air dry. This process

was repeated for a total of 3 coats, then the threads were heated at 100 C for 5 minutes to ensure dryness.

Chapter 3: Fabrication and Characterization of pH sensors

3.1 Fabrication

The pH sensors were fabricated by coating threads with inks, following the procedures outlined in Chapter 2. The working electrode was fabricated by coating the threads with 3 layers of stretchable carbon ink, curing on a hot plate at 90 ºC for 10 minutes after each coat. The coated threads were then dipped in the chilled PANI solution 3 times, held submerged for 1 minute while agitating the solution, and allowed to dry. After the final coat they were heated on a hot plate at 100 °C for 10 minutes to ensure complete dryness. Reference electrodes were made by coating the threads with silver/silver chloride ink 3 times and curing on a hot plate for 10 minutes at 120 ºC after each coat. Both thread types had Dupont connector pins crimped to the rear end of the thread, with the connection improved by a drop of the corresponding ink to the thread type.

3.2 Electronics and Code

To collect and analyze the voltage generated by the pH sensor, the working electrode is plugged into an analogue port on an Arduino board (Adafruit feather m0), while the reference electrode is connected to the board's ground.

Some initial problems were encountered in testing, such as excessive noise in the signal that made the sensors effectively impossible to use. The initial code was recorded and displayed raw, with no filtering or modification. In order to get rid of the noise, the data was put through a simple filter by averaging 10 measurements into one datapoint. This created smooth and useable data. The Arduino is Bluetooth equipped, and the code can be

configured to transmit the data wirelessly to a cell phone or via a wired connection to a computer.

3.3 Testing

The pH sensors were tested in phosphate buffered saline (PBS) solutions, made by dissolving one tablet of P4417 PBS from Sigma Aldrich in 200 mL of distilled water. The solution pH was then adjusted using HCl and NaOH to values between 4 and 8. The pH threads were placed in the solution, and the resulting readings transmitted via Bluetooth and recorded on a cell phone. Two primary elements of the pH sensors had to be evaluated; the accuracy and ability to distinguish between pH levels and the long-term stability during use.

3.3.1 pH measurement

The ability of the threads to measure pH accurately was tested by immersion in pH solution and recording the results over time. The first experiment, shown below in Figure 4, was performed by leaving a sensor in pH solution for 1 hour before removing it, rinsing, and placing in a new pH solution. This was performed in pH 5, 6, 7, and 8. The results indicate the sensors are effectively able to distinguish different pH levels in short term tests. Once the viability of the sensors was demonstrated, they were tested again by placing in pH solutions, but this time instead of recording the time-varying data, only the final value at each pH, after the readings had settled, was recorded. These values were used to plot a calibration curve, shown below in Figure 4, to determine the response of the sensors.

Literature indicates a theoretical voltage/pH slope of 62.4 [30], which is similar to the measured value of 54.3 mV/pH.

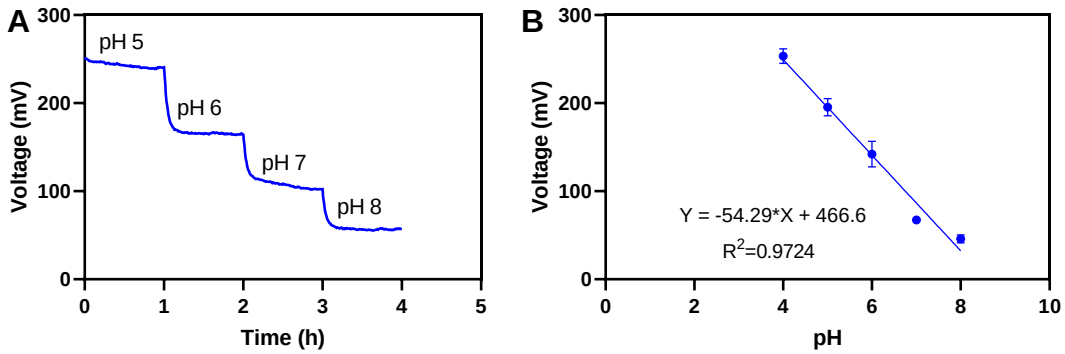

Figure 4: pH sensor measurement data. A) Showing short term tests over time, demonstrating the response of one sensor exposed to a changing pH. B) Final values of sensors in different buffer solutions, showing the overall response and calibration curve. Error bars indicate standard deviation, calculated from samples in triplicate.

3.3.2 Repeatability and response time

A second parameter that was tested was the hysteresis of the thread sensor. This was tested by placing the pH sensor in buffer solution at pH 7, then transferring to pH 6, and repeating. The result is shown below in Figure 5 and demonstrates that the sensor has a fast response time, settling within minutes, and returns the same value over repeated tests. Additionally, the slope of the response was plotted over time, showing that the response of the sensors flattens out to a constant value rapidly.

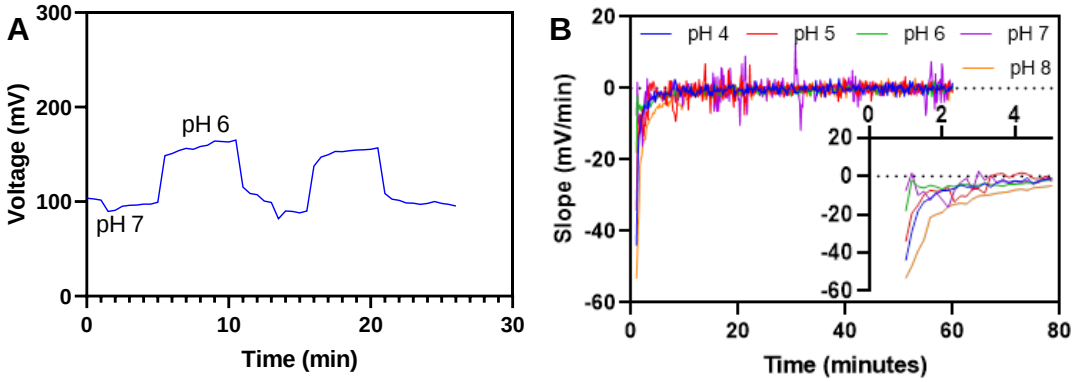

Figure 5: A) Repeatability test, showing that as the pH solution is switched, the sensor responds quickly and consistently. B) Response time test, showing that the slope of the pH response approached zero within a few minutes, and remained close to zero, demonstrating stability. The inset shows a closer look at the initial responses.

3.3.3 Stability

To test the stability of the sensor in solution, they were placed in pH buffer for 12-hour periods. The results show a drift of around 3.7% at pH 6 and 21% at pH 7 over 11 hours, but there is still an easily discernable difference between the pH values, shown below in Figure 6.

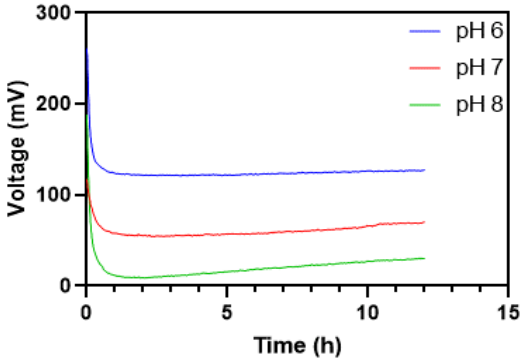

Figure 6: Stability test, showing the sensors in constant pH solution over 12 hours.

Chapter 4: Heating and Drug Release

The smart bandage is intended not only to measure pH and monitor the wound bed for infection, but also to deliver topical, on-demand antibiotics to halt infection in its early stages. The ability to detect infection in early stages and deliver high concentrations of antibiotics directly to the wound bed is integral to the purpose of the device. This is achieved using a thread-based heating element, with thermoresponsive drug releasing particles.

4.1 Fabrication

The heating threads were fabricated by coating with silver ink, as discussed in Chapter 2. Three such coats were applied, and the thread was cured for 10 minutes at 120 °C after each coat. Dupont pins were affixed to both ends of the threads with silver ink for conductivity, so that the thread could be placed in series within a circuit.

4.2 Electronics and Code

The heating thread acts as a heating element and undergoes Joule heating by the application of current. The heat generated is governed by the following equation, the general equation for power [31]:

$$P = IV = I^2R = \frac{V^2}{R} \tag{2}$$

Which assumes that all the power dissipated across the element is converted to heat. This equation states essentially that the energy dissipated across the element, converted to heat,

is the multiplication of the energy dissipated per charge (voltage, V) by the charge passing through the resistor per unit time (current, I).

The control system of the heating device uses a square pulse wave, produced by using the circuit shown below, in Figure 7. A power supply runs through the heating element, which is connected to a 30N06L high-power logic level N-Channel MOSFET (metal oxide semiconductor field effect transistor), that acts as a gate, preventing current flow except when it is activated by a signal at the gate that is generated by the Arduino microcontroller. When the MOSFET is activated, power flows freely across the heating element, then shut down to zero. The resulting power generated is a square wave pulse.

This is controlled by a PWM, pulse width modulator, on the Arduino. This allows control over the time that the MOSFET is open, by controlling the fraction of the time that the signal is applied to the MOSFET, known as the duty cycle. The Arduino PWM operates at 500 Hz.

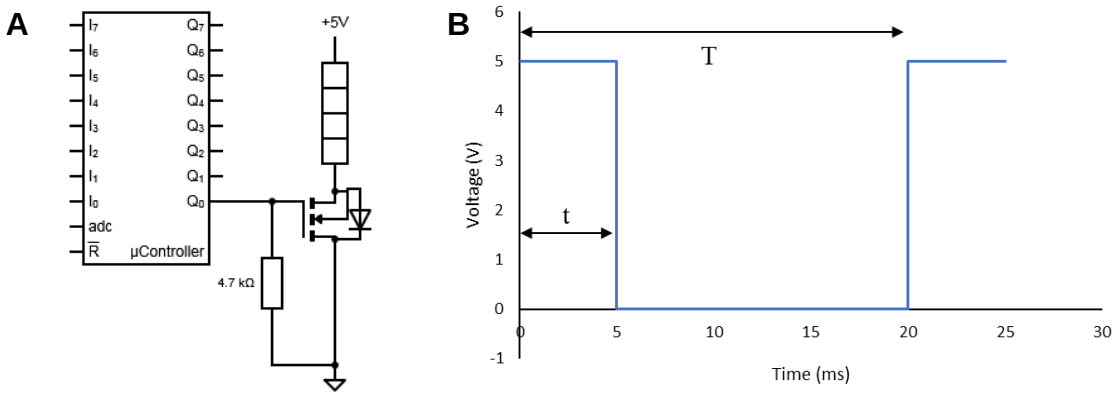

Figure 7: A) Circuitry of the heating element. A 30N06L MOSFET goes between the heating element and ground, allowing the pulse width modulator from the arduino to regulate the power delivered to the heater. B) The resulting 500Hz square wave of voltage produced across the heating element. The ratio of active time to total time, t/T, is called the duty cycle.

Equation (2) is for direct current systems and can be modified to function for alternating current systems as shown below.

$$P = V_{RMS} I_{RMS} = \frac{V_{RMS}^2}{R} \tag{3}$$

Where V_{RMS} is the root-mean square value of voltage, which is effectively the average voltage. It is defined by the following equation, assuming a square wave pulse [32].

$$V_{RMS} = \sqrt{\frac{1}{T}\int_0^T V(t)^2 dt} = V\sqrt{\frac{t}{T}} = V\sqrt{D} \tag{4}$$

Where D is the duty cycle of the square wave pulse, the fraction of time that the voltage pulse is active, and V is the peak voltage of the square wave. From this, the power equation, equation (3), can be rearranged in terms of duty cycle as shown below, in equation (5).

This is important, since the applied peak voltage remains constant in this system and duty cycle is the variable of interest.

$$P = \frac{V_{RMS}^2}{R} = \frac{V^2 D}{R} \tag{5}$$

This indicates a linear response to the duty cycle applied, as opposed to the quadratic response expected in terms of V_{RMS}.

4.3 Heating characterization

With the heating threads prepared, it was important to test the level of control possible on the threads. This is important because the drug releasing component requires a certain level of thermal stimulation to be effective, but excessive heat will become a health hazard and put the user at risk of burns. The heating of the thread was measured using a thermal camera from Seek Thermal, Inc. The thread and microcontrollers were fixed in place, and the thermal camera placed directly above the heating threads to measure the temperature, as shown below in Figure 8. The duty cycle of the PWM was adjusted to vary the power delivered to the heating element, and the resulting temperature change was measured with the thermal camera. To ensure accurate and comparable results, a heating pad at a fixed temperature of 100 ºC and a piece of ice at 0ºC were placed in frame, to control the min and max values of the colour scale used by the camera.

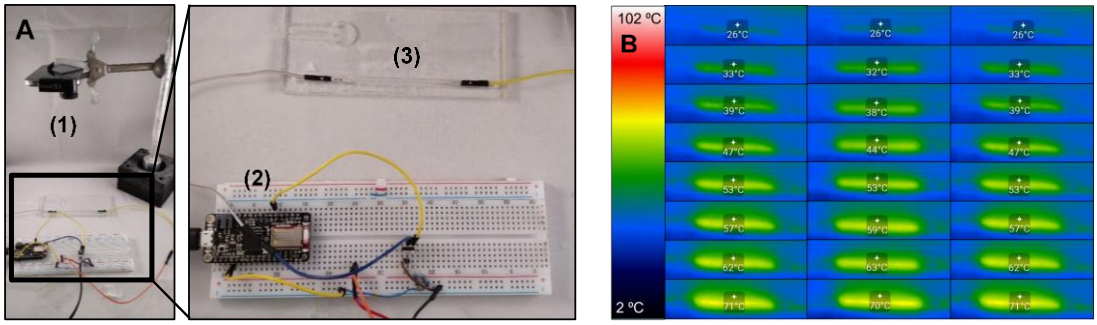

Figure 8: A) Experimental apparatus for the heating thread, to measure temperature at different duty cycles. Shows the thermal camera (1), Bluetooth device (2), and heating thread (3). B) Thermal images of heating thread at various levels of excitation

The results from this test are compiled below, in Figure 9, which shows that as the response curve with respect to duty cycle is, as expected from equation (5), a linear relationship. Additionally, when plotted with respect to RMS voltage a quadratic relationship emerges, again consistent with the equation.

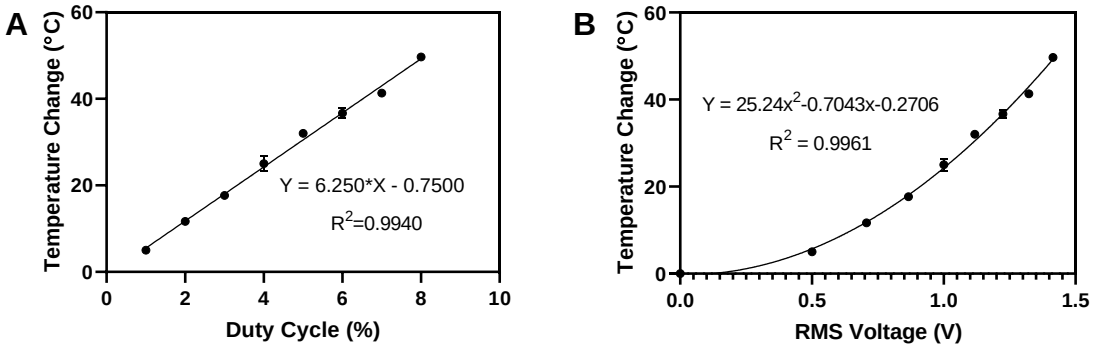

Figure 9: The heating element test results compiled and plotted, showing that the response with respect to A) duty cycle is linear and B) RMS voltage is quadratic. Error bars indicate standard deviation, calculated from samples in triplicate.

With the heating element and the pH sensors demonstrably effective, the next logical step became to connect the two. This was achieved by setting up both the pH sensors and the heating element on the Arduino at once. This done, the Arduino was programmed to activate the heating thread only if the pH fell below 6.5. Then, the pH sensors were placed in pH 7 solution, and the thermal camera set up to record video of the heating thread. The pH solution was removed and replaced with pH 6, causing the heating to activate. This process was repeated, demonstrating that the element can be turned on and off by stimulation with pH solution. The results from the thermal camera video were recorded and plotted in Figure 10, below.

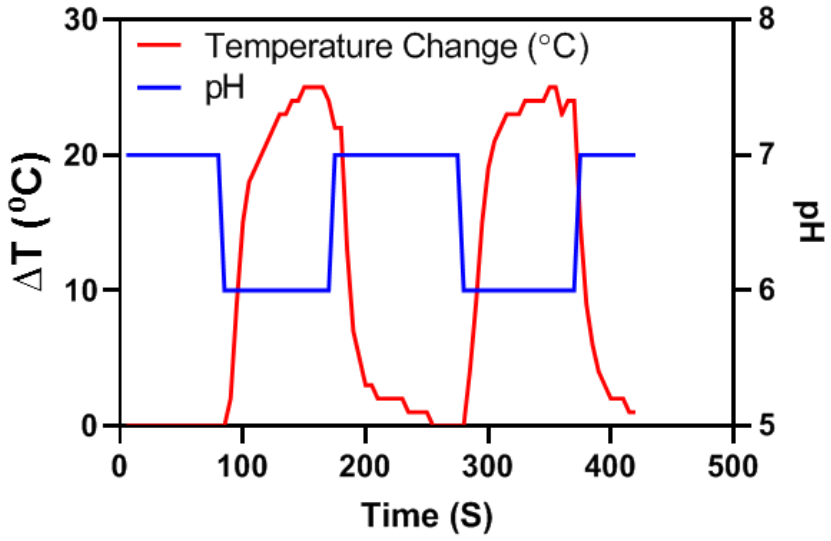

Figure 10: Plotted results of the pH sensor triggering the heating thread, showing that control over the heating element is effective.

Chapter 5: Drug releasing component

The heating thread was developed to trigger drug release from thermoresponsive particles. These particles are loaded with antibiotics, coated onto the heating threads, and when heated above a threshold activate and release the drugs they contain. For relevant data, statistical significance was determined using Welsh's t-test in GraphPad Prism. *P*-values are reported with the associated figures.

5.1 Chemical composition

The thermoresponsive polymer of choice for this project was poly-n-isopropylacrylamide, also known as PNIPAM. PNIPAM has a lower critical solution temperature, LCST, of 32 ºC. Below this temperature it exists in a hydrophilic, swollen state, but when heated above it transitions to a hydrophobic, shrunken state [33]. This characteristic makes it effective for the purpose of drug encapsulation and controlled release, as it can be formed into microspheres that will hold drugs and release them as needed, as in another work by Bagherifard et al [34]. The thermoresponsive characteristic of PNIPAM is not definitively understood, but is thought to be dictated by the balance of hydrophobic and hydrophilic properties of the polymer side chains [33]. As a result, the LCST can be modified by co-polymerization with other compounds. This is important, as the LCST of pure PNIPAM is too low for on-skin applications, which will routinely exceed 32 °C. Co-polymerization with poly(ethylene glycol) diacrylate, PEGDA, was used in this case to increase the LCST.

5.2 Particle fabrication

Following the previous work by Bagherifard et al [34], an aqueous dispersed phase was prepared containing PEGDA (20 wt%), NIPAM monomers (10 wt%), 2-hydroxy-4'-(2-hydroxyethoxy)-2-methylpropiophenone as the photoinitiator (1 wt%), N,N-methylenebisacrylamide (MBA) (0.4 wt%), and ammonium persulfate (APS) (0.6 wt%). A microfluidic flow-focusing device, shown below in Figure 11, was produced from poly-dimethyl siloxane (PDMS), and bound to a glass slide by plasma treatment. The main channel dimension of the microfluidic device was 500 μm, and the focusing channel was 90 μm. Heavy mineral oil containing 10% (v/v) span80 as non-ionic surfactant was used as the continuous phase, which was flowed into the junction with the aqueous phase to produce microspheres, as shown below in Figure 11. The aqueous phase passes through the focusing channel, and the incoming oil flows pinch off droplets of the PNIPAM solution into microspheres. The oil flow rate was kept at 25 μL/min, and the aqueous phase flow rate was kept at 2.5 μL/min, controlled by Harvard Apparatus PHD 2000 syringe pumps. The resulting flow is pumped through a spiral of tubing and exposed to UV light at 20 mW/cm^2 for 15 minutes. The curing process was performed on ice in order to prevent over crosslinking.

The produced particles are suspended in oil and must be extracted. This was accomplished by centrifuging the microparticles in Eppendorf tubes until settled, pipetting out the oil, and rinsing with Tween 20 in distilled water. The centrifugation and rinsing was repeated 3 times with pure distilled water, yielding clean particles.

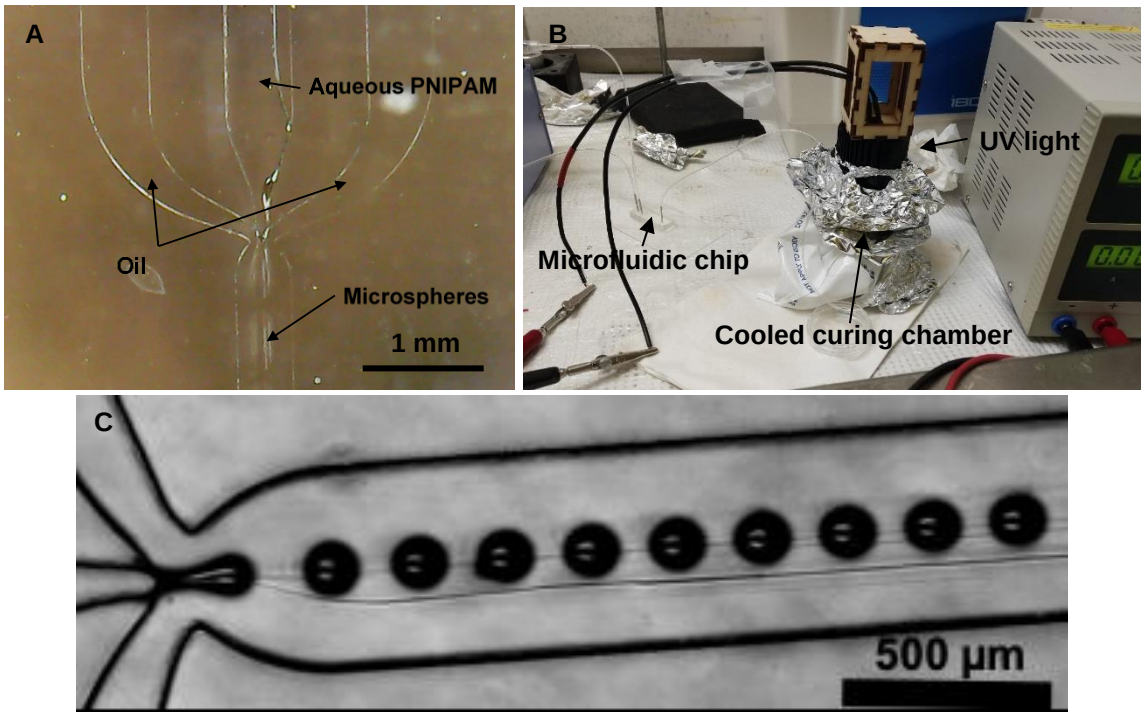

Figure 11: A) Microscope image of the microfluidic device. B) the fabrication set up, showing the microfluidic device, UV light, and cooled curing chamber. C) Bright field microscope image of the device and particles.

The particles were analyzed with Fourier Transform Infrared Spectra (FTIR), to confirm the chemical composition. This was performed using a Perking Elmer spectrometer between the wavelengths of 400-4000 cm^{-1}. The samples were prepared by grinding and powdering the lyophilized particles, then mixing with KBr and pressing them into a disk. The results, shown below in Figure 12, show that the characteristic peaks of PNIPAM (1543 cm^{-1} shows N-H bending, 1655 cm^{-1} indicates C=O stretching, and 3291 cm^{-1} shows secondary amide N-H stretching) and PEGDA (1100 cm^{-1} showing the C-O-C bond of ethylene glycol, 1732 cm^{-1} the C=O stretching from ester bonds due to acrylic groups, and 2882 cm^{-1} resulting from the C-H stretching vibration) are present in their respective

polymers, demonstrating that the copolymerization process was effective. Slight drift from the expected values can be attributed to interactions between the materials.

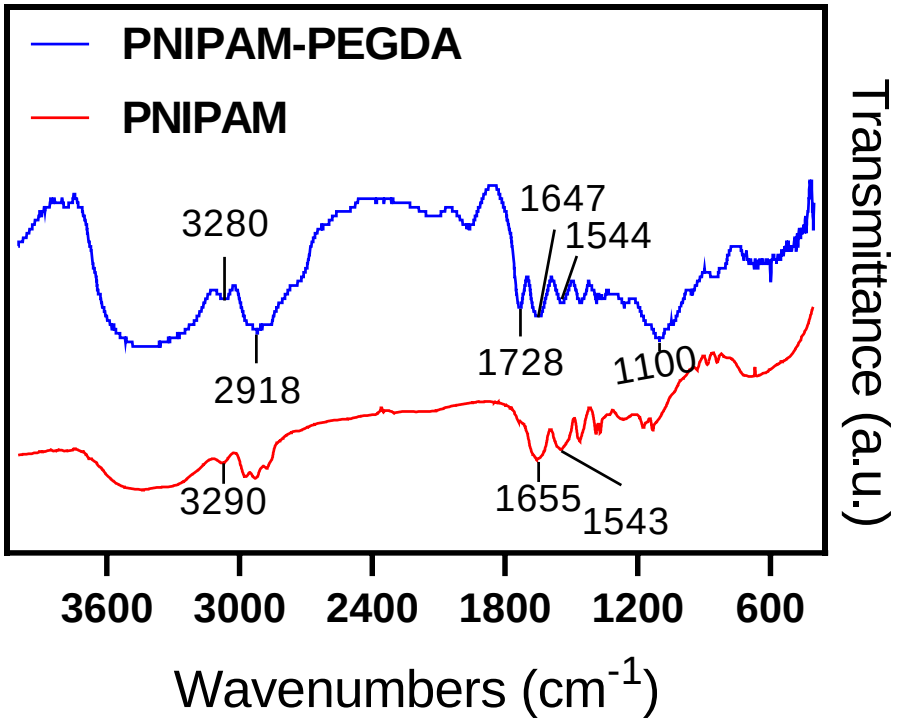

Figure 12: FTIR spectra of the microparticles

5.2.1 Size distribution

To determine the efficacy of the microfluidic chip and formation process in general, the particles were collected and imaged with a Zeis Axio Observer microscope. The size distribution of the particles was gathered from these images, as shown below in Figure 13, by analyzing with ImageJ. The PEGDA copolymer particles were smaller than pure PNIPAM particles made with the same conditions, because the addition of PEGDA changes the viscosity of the aqueous phase, causing it to split off into particles more quickly. The polydispersity index, or PDI, is low for both PNIPAM and PNIPAM-PEGDA

particles, 0.08 and 0.05 respectively, indicating reliable uniformity. Polydispersity index is defined by the equation below [35],

$$PDI = \frac{\sigma}{D_m} \tag{6}$$

Where σ is the standard deviation of the microsphere diameter, and D_m is the mean microsphere diameter.

This shows that the microfluidic device provides control over the size and uniformity of the particles produced, an improvement over other fabrication systems such as batch emulsion [36].

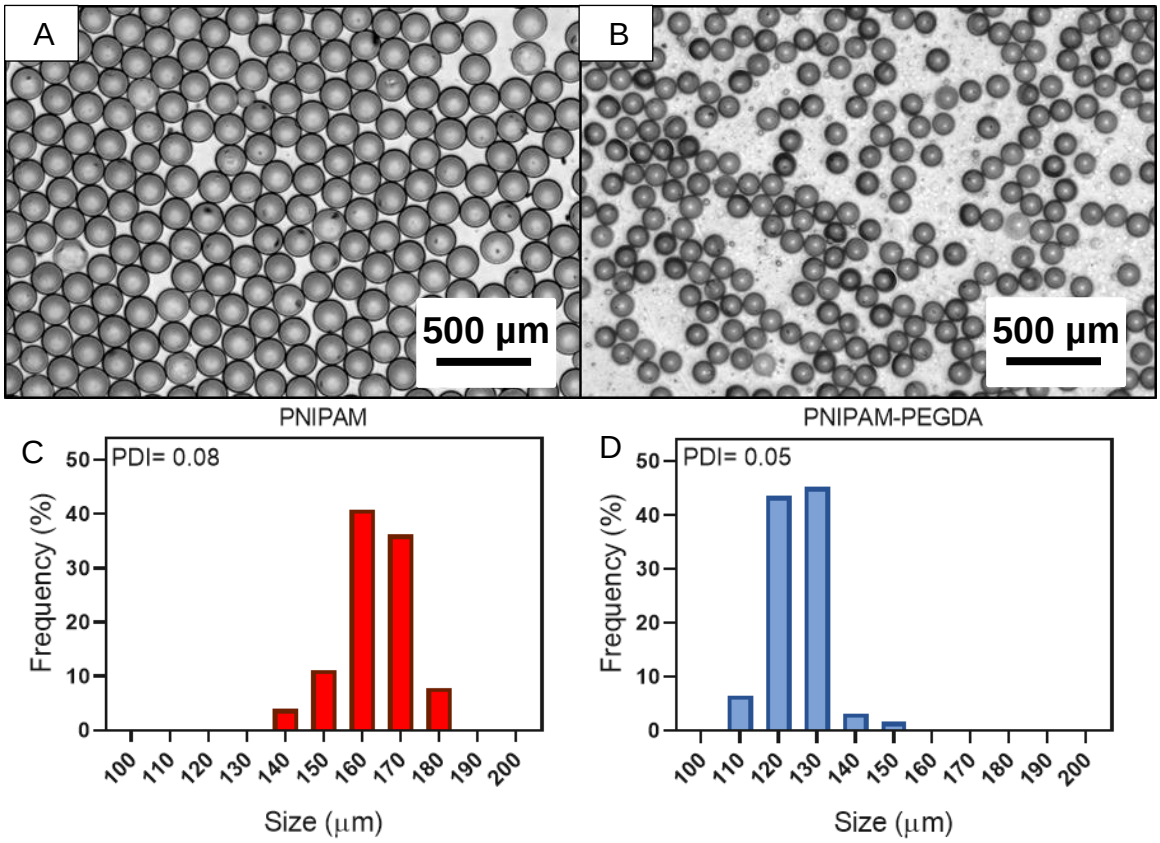

Figure 13: A) PNIPAM particles, B) PNIPAM-PEGDA particles, C) PNIPAM particle size analysis of 282 particles, showing a PDI of 0.08, D) PNIPAM-PEGDA size analysis of 186 particles, showing a PDI of 0.05.

After determining that the particles displayed acceptable uniformity, the next step was to observe and confirm the thermal response. This was performed by placing the particles on a hot plate at room temperature and setting up a Jiusion digital microscope to image the particles. The hot-plate temperature was then increased at a rate of 2 ºC/min, from room temperature to 42 ºC, while filming the particles through the microscope. The size change was imaged and plotted, as shown in Figure 14 below.

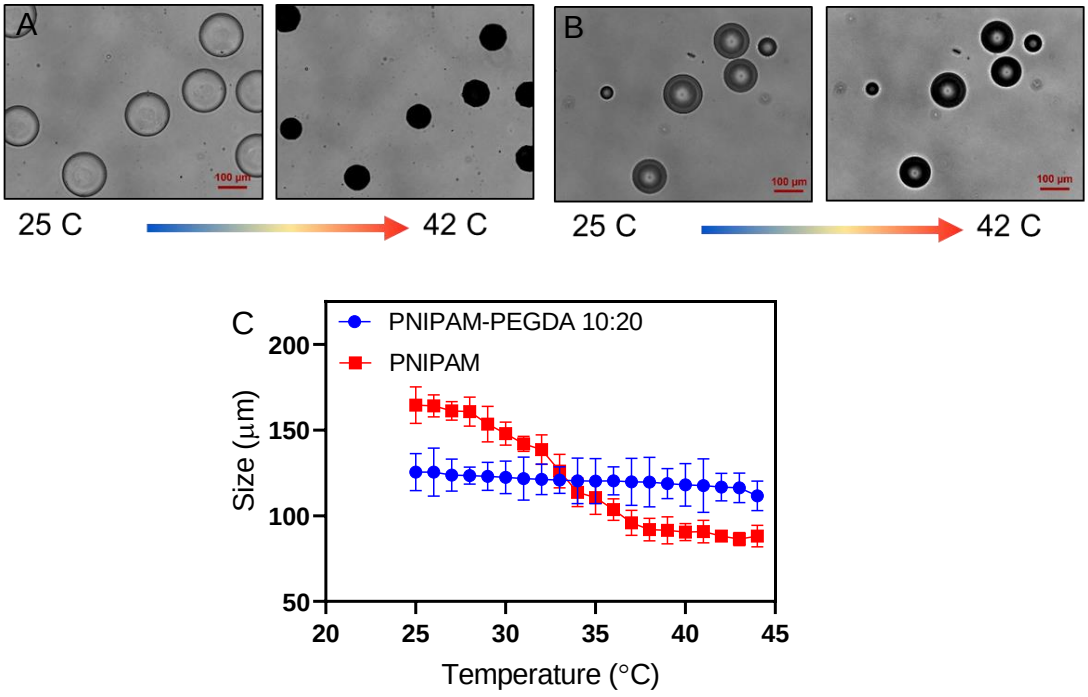

Figure 14: Size response of microparticles. A) PNIPAAM particles, B) PNIPAM-PEGDA particles, C) Particle size response plot. Error bars indicate standard deviation, calculated from samples in triplicate.

5.2.2 Loading and alginate dispersal

Ciprofloxacin hydrochloride is an antibiotic that is effective against gram-negative bacteria, and has a molecular weight of 331.34 g/mol [37]. It was dissolved in water to form a 1 mg/mL solution. PNIPAAM-PEGDA microspheres were collected and freeze-

dried to remove any water, then incubated in the ciprofloxacin solution at 4 °C for 48 hours. The low temperature caused the particles to swell, enhancing the uptake. The particles were then rinsed with distilled water 4 times to remove any surface bonded ciprofloxacin.

5 mg of drug loaded PNIPAM-PEGDA beads were loaded with ciprofloxacin according to the method described above and dispersed in 100 μL of alginate 2% (w/v) solution to obtain a suspension of particles with the ratio of 5% (w/v). To coat on threads, the resulting suspension was cast into a cylindrical PDMS mold with the conductive thread placed through the middle of mold. The material was crosslinked by placing a solution of 2 % (w/v) CaCl2 on top of the mold for 10 minutes. Finally, the coated thread was washed several times in distilled water to remove remaining calcium ions and other impurities.

In order to image the resulting dispersion on threads, a batch of particles was loaded with FITC-dextran, a fluorescent die. The resulting fluorescent image, obtained with a Zeis axio observer microscope, is shown below.

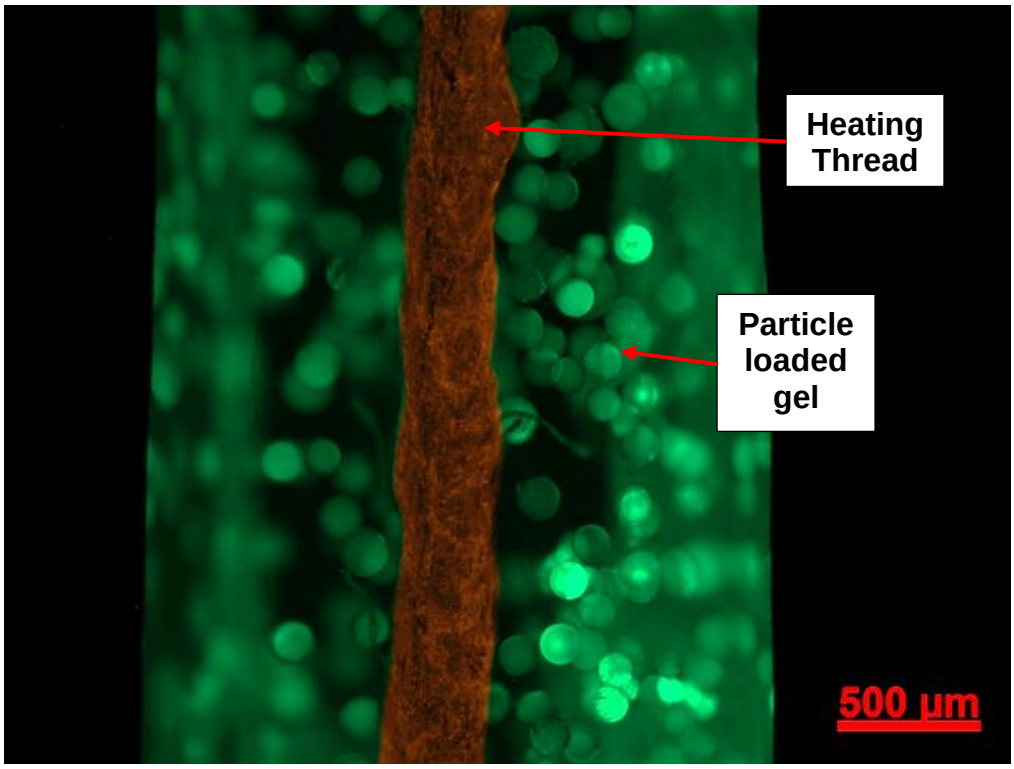

Figure 15: FITC-Dextran loaded in PNIPAM-PEGDA particles, suspended in alginate and coated on a heating thread. Particles shown in green, thread false-coloured orange.

5.3 Release Studies

Release studies were performed with both loose particles and with loaded threads. The release studies were performed by placing 5 mg of loaded particles in 1 mL of tris buffer kept at 25, 37 or 42 ºC, and extracting the buffer solution at timed intervals and measuring the concentration of ciprofloxacin in the supernatant by fluorescence excitation, using a Tecan Infinite M Nano plate reader. The resulting fluorescence intensity is converted to concentration using a calibration curve, producing the plots shown below in Figure 16. The experiment was repeated using threads coated with loaded particles. This was also conducted with PNIPAM-PEGDA copolymer microparticles. The particle release was

found to be generally faster than thread release, especially at room temperature, because the alginate coat acts as a barrier. In addition, a strong burst release was observed, followed by a gradual flattening. This behaviour was slowed in the alginate coated threads. The release at body temperature, 37 ºC, was found to be unacceptably high in PNIPAM particles, but was significantly lowered in PNIPAM-PEGDA copolymers.

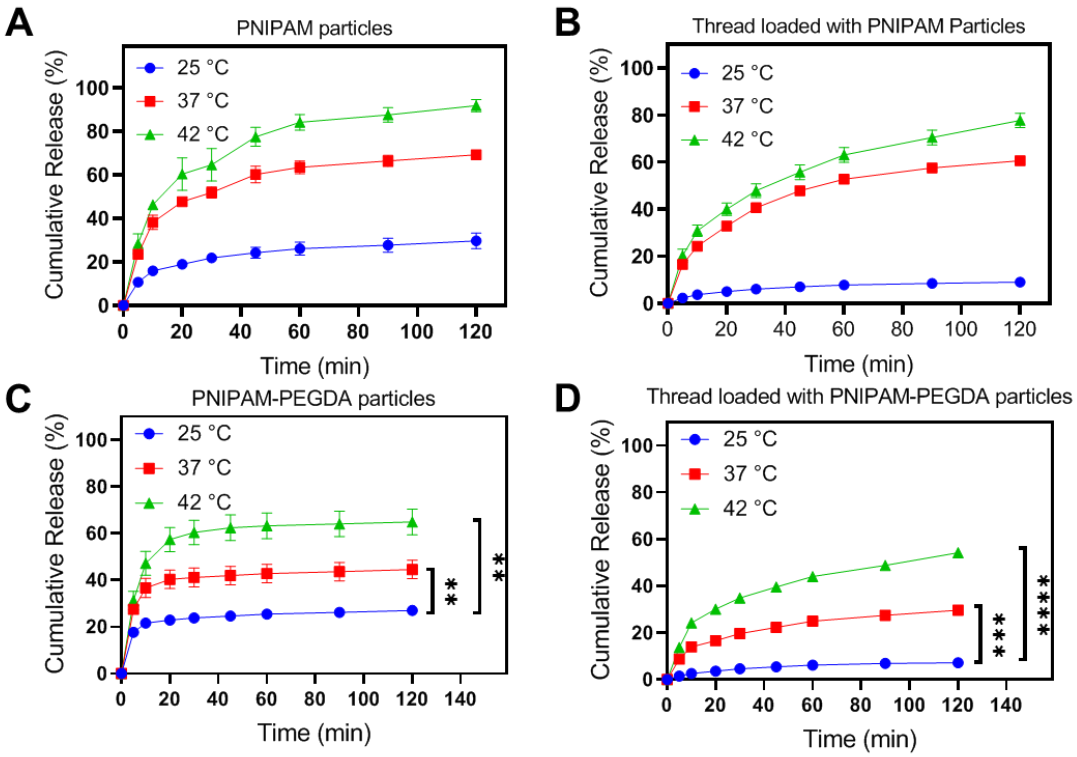

Figure 16: The PNIPAM and PNIPAM PEGDA release studies, performed in Tris Buffer. A) PNIPAM particles loose in buffer solution, showing high release at 37 ºC. B) PNIPAM particle loaded threads in buffer solution, showing high release at 37 ºC. C) PNIPAM-PEGDA particles loose in buffer solution, showing lower release at 37 ºC. D) PNIPAM-PEGDA particles loaded on threads in buffer solution, showing lower release at 37 ºC. (Error bars indicate standard deviation, calculated from samples in triplicate. *P*-values: *<.1, **<.01, ***<.001, ****<.0001)

To evaluate the effectiveness of the system for delivering on demand antibiotics, a pulsatile release experiment was performed. This was conducted by immersing a loaded heating thread in 2 mL of tris buffer and applying heating and cooling cycles using the Arduino. The thread was heated for a 5-minute cycle, and then left to cool for 25 minutes. The supernatant was collected at the end of each cycle of heating or cooling, and the concentration of ciprofloxacin was measured as described previously. The results, shown below in Figure 17, show that the release is triggered when the heating is activated, but flattens out when left at room temperature.

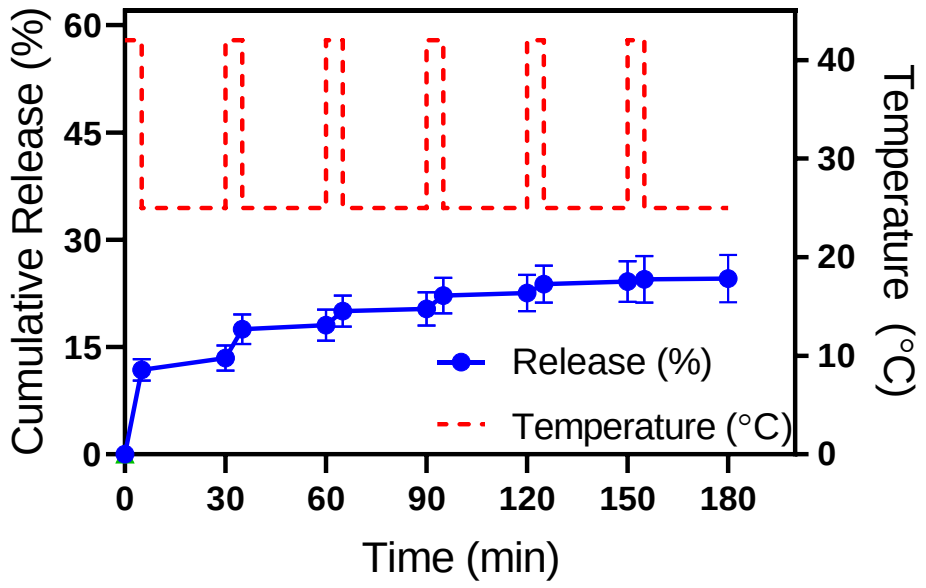

Figure 17: Pulse release of ciprofloxacin loaded particles coated on threads and heated for 5-minute bursts. Error bars indicate standard deviation, calculated from samples in triplicate.

Chapter 6: Bacterial and Animal Studies

Once the components of the device—the pH sensor and the drug releasing thread—were prepared, tests were performed on Escherichia Coli (*E. coli*, W3110, ATCC9637) and on mice. The animal work was conducted on behalf of this project by Zhina Hadisi, a PhD student also working under Dr. Akbari. These were conducted to demonstrate that the device is effective at detecting and killing bacterial infection, and that it is safe and effective at promoting healing. For relevant data, statistical significance was determined using ANOVA. *P*-values are reported in the associated figures.

6.1 Bacteria work

The bacteria used, *E. coli*, is common in burn wounds [12]. Experiments were performed either on *E. coli* cultured in a nutrient broth or grown on agar plates. For preparing broth, 2 colonies of *E. coli* were harvested and dissolved in 5 mL of Luria-Bertani (LB) broth (Fisher Scientific, CAT#DF0402-17-0), then left to culture for 24 hours in 37 °C. The solution was then aliquoted, 100 µL in 5 mL of LB broth, and allowed to culture for 1 hour, before withdrawing 50 µL and aliquoting in 5 mL of broth. This produces a solution with a concentration of 10^8 CFU/mL. To prepare agar plate samples, one line of *E. coli* was collected, and dissolved in 1 mL of LB broth. 100 µL of this solution was then deposited on an LB-agar plate and spread evenly over the surface.

6.1.1 pH measurement

The first tests performed were to examine the effectiveness of the pH sensitive thread for measuring bacterial growth. By culturing *E. coli* in broth at 37 ºC and measuring the pH of

the solution with pH sensitive threads, the pH curve of *E. coli* over the first 7 hours of culture was prepared as shown below in Figure 18. The CFU concentration was also measured, using the plate reader and the McFarland Standard method [38].

The two values are plotted below, showing that the pH decreases over time. When the bacterial growth begins to increase rapidly, after about 5 hours, the pH drops to 6.5. As a result, in further studies this pH was used as the trigger point to indicate the presence of a substantial, growing population of *E. coli.*

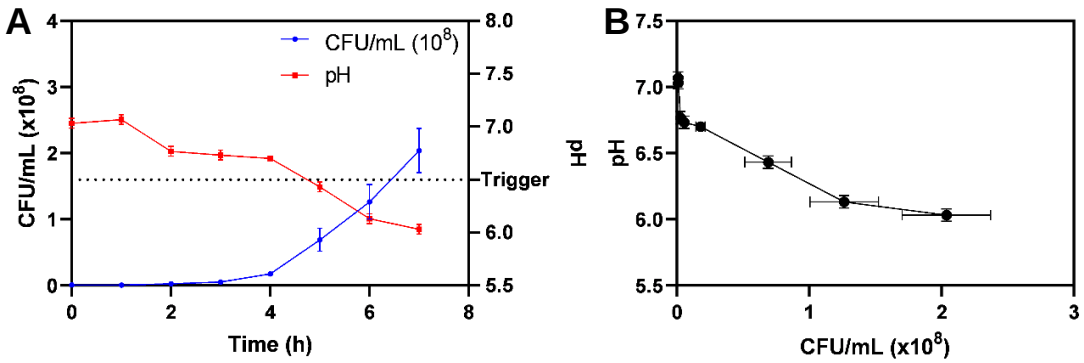

Figure 18: Detailed analysis of the first 7 hours of bacterial culture, showing A) CFU and pH over time, and B) pH compared to CFU. Error bars indicate standard deviation, calculated from samples in triplicate.

6.1.2 Antibiotic delivery in broth

To test the effectiveness of the antibiotic delivery system, the heating thread with ciprofloxacin loaded PNIPAM-PEGDA microparticles suspended in alginate coated on it, was used in a series of experiments with *E. coli* in broth and on agar plates. The first two experiments were conducted in broth. As shown below in Figure 19, bacteria was cultured in LB broth and the supernatant was collected after 2 hours of growth and analyzed in the plate reader. Then, the bacteria was subject to 4 conditions; a control group with no

modification, a group where an unloaded heating thread was placed in and activated for 5 minutes, and two groups with drug loaded heating threads, one activated for five minutes and one left inactive. The threads were then removed, and the samples left at 37 °C to culture overnight. Following this, the samples were analyzed for CFU concentration by the plate reader. The results indicate that, while heating alone had no impact on the bacterial growth, the drug releasing threads, when activated, reduced bacterial growth by half.

Having demonstrated that the drug releasing thread was effective, the integration of the pH sensor and the drug releasing thread proceeded, as shown below in Figure 19. This was achieved by culturing the *E. coli* in broth, while a drug releasing thread was placed in tris buffer. The drug releasing thread was configured to heat and activate only when the measured pH fell below the previously determined value of 6.5. Measurements of pH and ciprofloxacin release were taken every 2 hours, and the pH fell below 6.5 at the 6-hour mark, causing a spike in the measured drug release, thus demonstrating the effective integration of the pH sensor and drug releasing element.

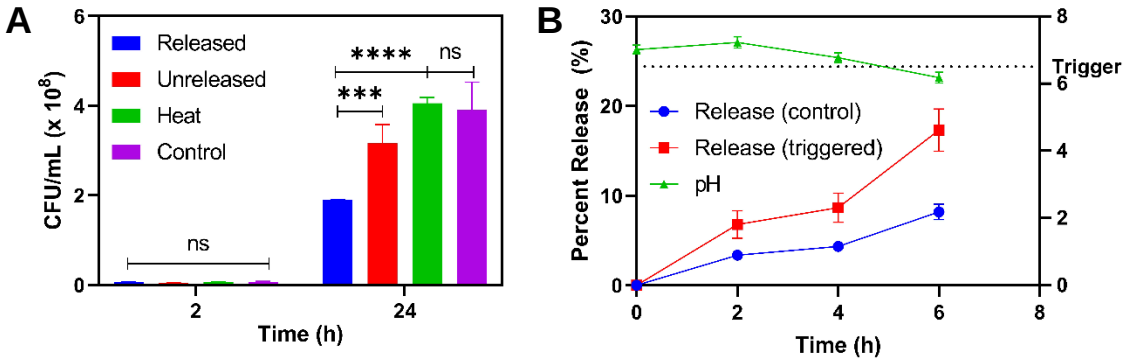

Figure 19: A) demonstrating ciprofloxacin releasing thread effectiveness at inhibiting *E. coli* growth. Threads subject to heating experienced much lower bacterial growth than control samples. Error bars show standard deviation. B) Demonstration of the integrated pH sensor and drug delivery. pH measurement of *E. coli* growth triggers drug release after 6 hours. (Error bars indicate standard deviation, calculated from samples in triplicate. *P*-values: *<.1, **<.01, ***<.001, ****<.0001)

6.1.3 Antibiotic delivery on agar plates

The next test was performed on agar plates, demonstrating the topical effectiveness of the delivery. A 2% agar solution was made using LB broth and poured into a petri dish to form a uniform layer. For this experiment, an *E. coli* monolayer was produced on an agar/LB broth plate as described previously. Drug loaded threads were then placed on the agar plate and triggered for different times, and a blank alginate coated thread was placed on the plate and heated for 5 minutes. The threads were then left on the plates for 24 hours to allow the bacteria to culture, and the zone of inhibition measured. The results are shown below in Figure 20.

The drug releasing threads created a zone of inhibition around the threads, where *E. coli* was unable to grow. The zone of inhibition was larger, the longer the thread heating was on. The heated blank thread produced no zone of inhibition, indicating that the heating

itself had no effect. Swabs taken from areas within the zone of inhibition showed no growth after 24 hours of culture in 37 ºC, while swabs from close to the edge had very little growth and a swab from the edge produced numerous colonies. These results indicate that the drug

releasing threads are effective for topical drug delivery, and that prolonged heating produces a larger zone of inhibition.

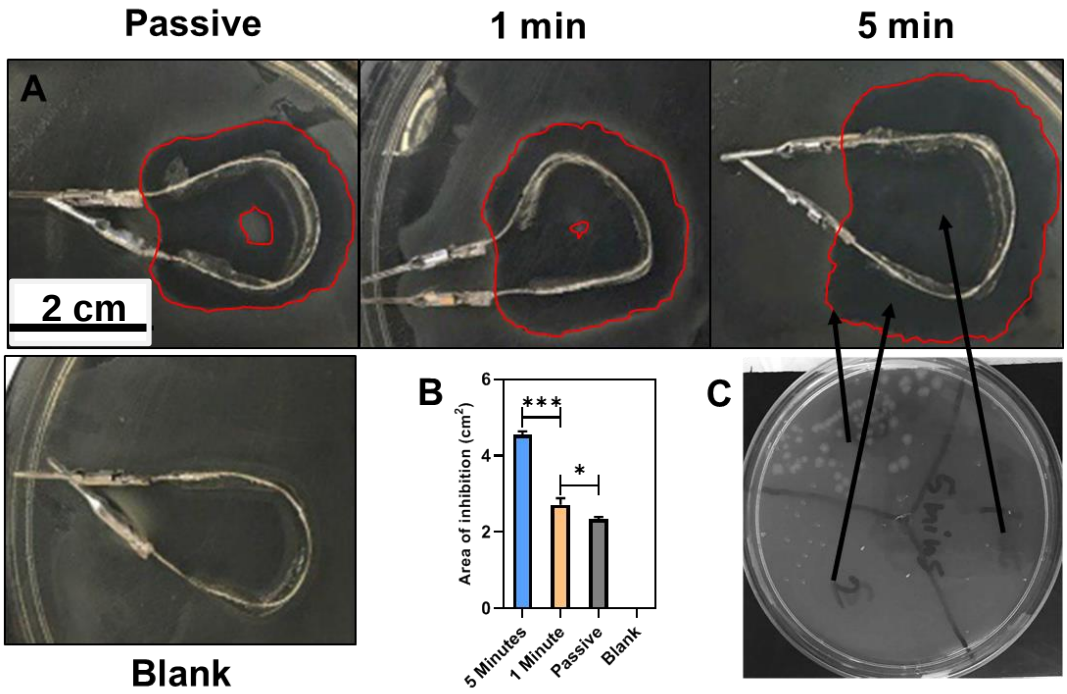

Figure 20: Ciprofloxacin release on agar plates. A) Representative samples of the zone of inhibition produced at different levels of heating, zone of inhibition outlined in red for clarity. B) Overall zone of inhibition results, showing control over the area affected by the drug, (Error bars indicate standard deviation, calculated from samples in triplicate. *P*-values: *<.1, **<.01, ***<.001, ****<.0001) C) Cultured swabs showing effective anti-bacterial action within the zone of inhibition.

6.2 Animal Studies

The body is a complex organism, so studies in test tubes and petri dishes are not an effective analogue for an actual wound. For this reason, in addition to the bacterial work, experiments were conducted on BALB/c mice. Mice have some unique and different anatomical features and healing mechanisms compared to humans such as the *panniculus*

carnosus muscle layer [39], but are nevertheless an effective analog to humans for studying the process of wound healing and modeling treatments [40], [41]. Because this work compares the relative healing of mice—all equipped with the same natural mechanisms but subject to different treatments—the result, expressed as an improvement in healing outcomes, should be relevant. The mice used were six weeks old, male, and weighed between 20 and 30 g. The mice were acclimatized for one week before conducting experiments.

All animal work was performed following the policies and procedures of the Animal Care Committee at the University of Victoria. Before procedures, the animals were anesthetized with inhaled isoflurane (2%), after which the dorsal surface was shaved with clippers and dried. Two parallel wounds were then induced with an Integra Miltex® biopsy punch, with diameters of 6 mm, and photographed [42]. Next, the mice were divided into the following three groups: no treatment, blank heating threads, and drug loaded threads. Seven days after the initial injury the mice were euthanized by cervical dislocation, the wound dressings removed, and the wounds were imaged to calculate wound closure according to the following formula [43]:

$$\text{Wound closure (\%)} = \frac{A_0 - A_t}{At} \times 100 \quad \textbf{(7)}$$

Where, A_0 and A_t are the initial wound area and the wound area at time t, respectively.

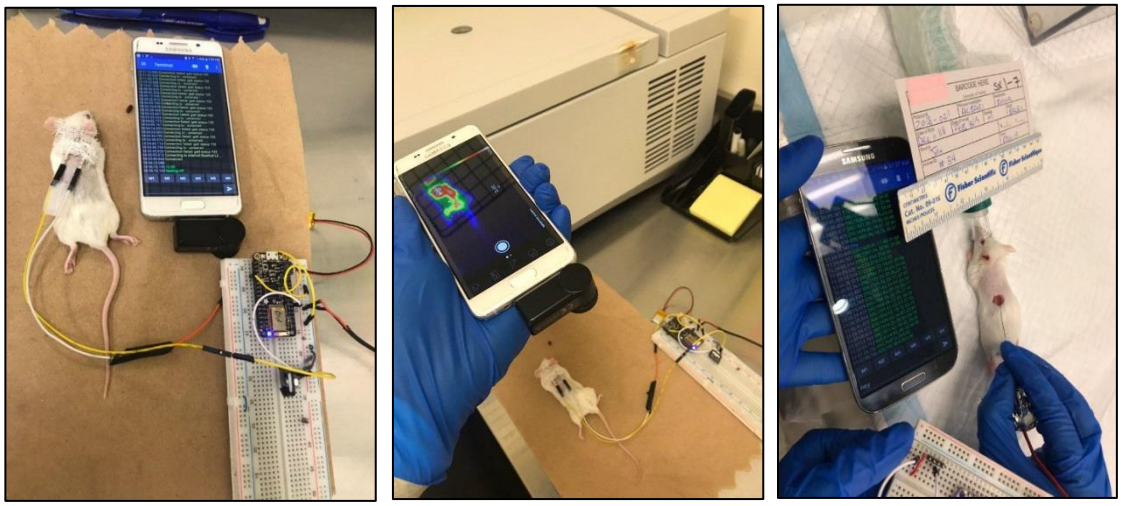

Figure 21: Animal study work, showing from left to right: drug-releasing thread on wound, thermal imaging of drug releasing thread, pH sensing on wound

The wound contraction was measured for all groups at day 7 post-injury, as can be seen from Figure 22 below. The wound closure of both the thread treated groups was significantly higher than that of the control group (no-treatment). Wound contraction in the no-treatment group was around 16.67±1.28%, while the unloaded thread and ciprofloxacin loaded thread-based wound dressings led to 22.86±1.89% and 43.96±2.51% wound closure respectively. This was significantly higher than the wound closure observed in no-treatment groups ($p^* < 0.05$). This means that mice treated with threads containing ciprofloxacin showed the fastest healing rate among all groups. Based on these results, it can be concluded that the alginate-ciprofloxacin threads can effectively avoid providing substrate for bacterial growth and consequently reduce the risk of wound infection. The beneficial effects of antibacterial compounds such as ciprofloxacin on the wound healing process have been demonstrated in the past [44], [45].

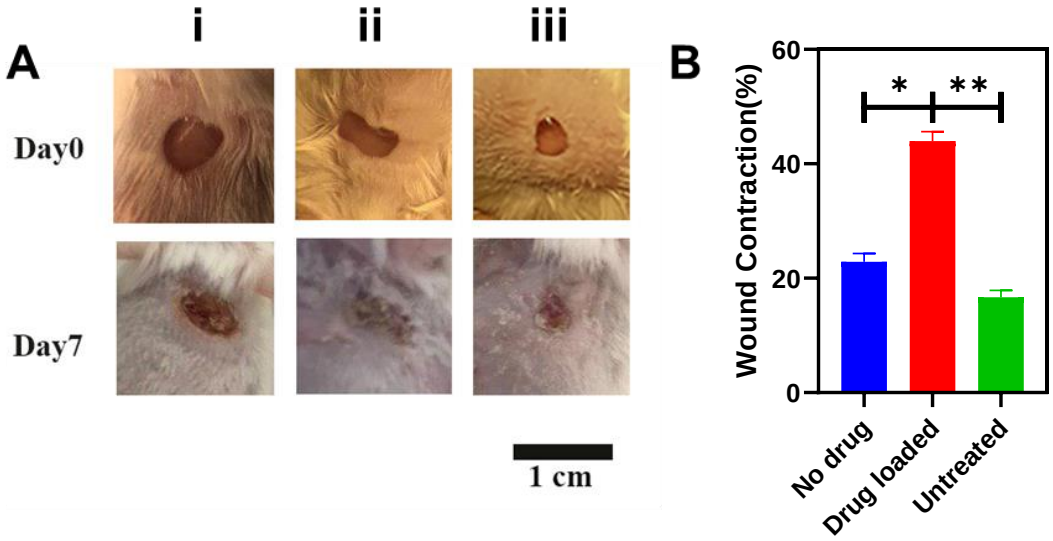

Figure 22: A) i) untreated wound, ii) wound treated with blank threads, iii) wound treated with drug loaded threads. B) Wound contraction percentage. (Error bars indicate standard deviation, calculated from samples in triplicate. *P*-values: *<.1, **<.01, ***<.001, ****<.0001)

6.2.1 Histopathological staining

The wounds were also subjected to histopathological analysis to further analyze the healing effects of the drug releasing threads. Tissues from the different wound groups were collected and fixed in buffered formalin (10%). These were then transferred to a 30% sucrose solution for slicing. A Leica CM1850 UV cryostat was used to collect 5 µm sections, which were then treated with Bouin's Solution and stained with Hematoxylin and Eosin (H&E) and Masson's trichrome (MT) staining. H&E staining is used routinely in histopathology laboratories as it provides the pathologist/researcher a very detailed view of the tissue. It achieves this by clearly staining cell structures including the cytoplasm, nucleus, and organelles and extra-cellular components. MT staining on the other hand is useful for showing collagen, which is important since collagen is the main component of

skin extra cellular matrix [46]. The stained sections were finally analyzed under an Olympus BX51 light microscope.

The results of this analysis, shown below in Figure 23, show that the wound dressing improves healing outcomes. According to the H&E staining, the control treatment group showed poor healing, with dermis damage, disorganized collagen fibers and prominent inflammatory cell infiltration, as visible in the figure shown below. The unloaded heating thread showed better results, with evidence of re-epithelialization and more organized collagen fibers, with tissue granulation and fibroblast activity. However, inflammatory cells were still present. The drug loaded treatment group showed the best results, presenting a thicker epidermis with a clear distinction between the dermis and epidermis. The drug treated group also presented greater neo-vascularization, more organized and dense connective tissue, and lower levels of inflammatory cell infiltration.

The MT staining result, which emphasizes collagen, shows a similar result. The collagen deposition is both more organized and more prominent in the drug treated group as opposed to both the control and blank.

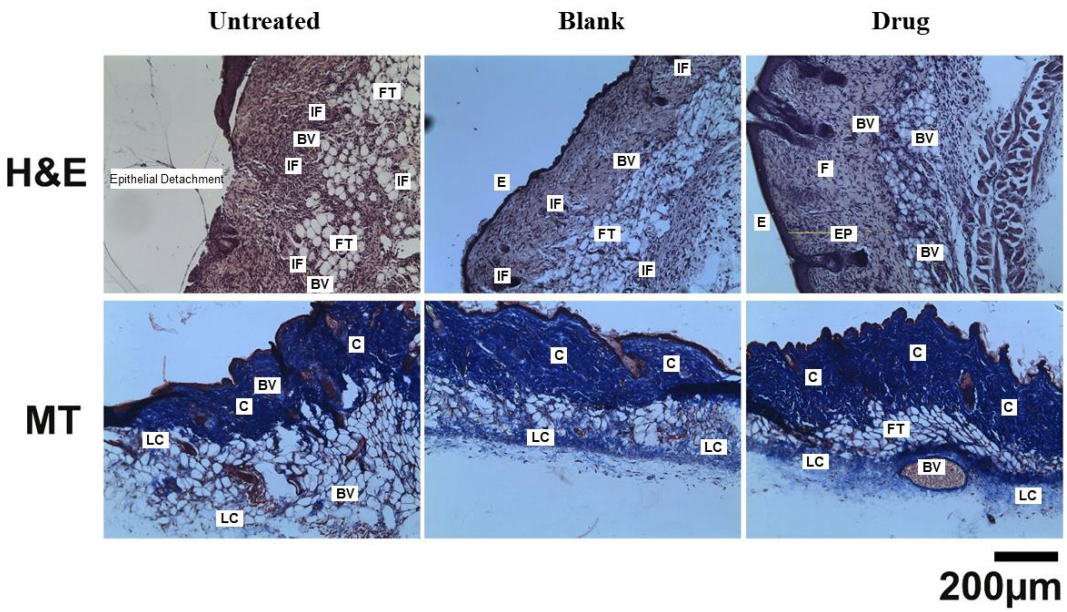

Figure 23: The H&E and MT pathological images of the wound sites treated with different groups after a 7-day treatment. Overall, this shows much better and more natural healing in the group treated with the drug releasing thread. ((H: hair follicles; BV: blood vessels; EP: epithelialization; IF: inflammatory cells; F: fibroblasts; C: collagen; LC: loose collagen; E: new generated epidermis; FT: fatty cells)

Conclusion and Future Work

This wound dressing developed here is an effective tool for monitoring and treating infection at the wound site, without requiring intervention that can be unpleasant and unsafe. The device can be especially effective for burn wounds and chronic wounds and is designed to be effective for both hospital and home care applications. The thread-based construction of the device provides flexibility and versatility, and the sensors and drug delivery systems are effective at detecting and eradicating bacteria.

The pH threads are a flexible and versatile tool that can be shaped or sewn into myriad shapes, and can be used to electrochemically detect pH, and therefore infection, in wounds. They are simple to produce and use, and have effective pH monitoring characteristics such as precision, response time and stability. However, some issues and challenges still exist for the pH sensors.

- The freshly fabricated sensors must be left in pH buffer overnight to reach an equilibrium before they can be used. The initial response time is large, several hours, but after this treatment it drops to seconds or minutes.
- There is significant batch-to-batch variation in the response values of the thread sensors. This means that each thread or batch of threads must be calibrated before it can be used. This issue could be resolved by introducing more stringent quality control measures.

Heating threads are an effective, flexible and easily manufactured tool for delivering thermal energy to a target. The control system developed allows for effective control over these heating threads in accordance with the pH sensors. PNIPAM-PEGDA microparticles

with effective thermoresponsive properties were also produced and coated on threads, demonstrating effective drug release in response to heating.

The bacterial work and animal studies conducted both illustrate the effectiveness of the wound dressing. Bacterial growth was successfully used to trigger drug release, which was in turn effective at inhibiting *E. coli* growth. In addition, the wound dressing had positive effects on the wound healing on mice.

The next steps with this design include plans to incorporate temperature sensitive threads to provide better feedback and analysis on the wound-bed and to establish a feedback loop for the drug delivery heating thread. Additionally, improving the system to contain a network of drug-eluting threads could allow control over, and delivery of, several different drugs according to the nature of the infection detected, and would allow for higher specificity and broader application.

Bibliography

[1] K. F. Cutting, “Identification of infection in granulating wounds by registered nurses,” *J. Clin. Nurs.*, vol. 7, no. 6, pp. 539–546, 1998.

[2] S. Ono, R. Imai, Y. Ida, D. Shibata, T. Komiya, and H. Matsumura, “Increased wound pH as an indicator of local wound infection in second degree burns,” *Burns*, vol. 41, no. 4, pp. 820–824, Jun. 2015.

[3] J. Santy, “Recognising infection in wounds,” *Nurs. Stand.*, vol. 23, no. 7, pp. 53–60, Oct. 2013.

[4] CIHR, “Compromised wounds in Canada: Executive Summary,” 2013.

[5] A. Kingsley, “The wound infection continuum and its application to clinical practice.,” *Ostomy. Wound. Manage.*, vol. 49, no. 7 A Suppl, pp. 1–7, 2003.

[6] P. G. Bowler, B. I. Duerden, and D. G. Armstrong, “Wound microbiology and associated approaches to wound management.,” *Clin. Microbiol. Rev.*, vol. 14, no. 2, pp. 244–69, Apr. 2001.

[7] R. Bamberg, K. P. Sullivan, and T. Conner-Kerr, “Diagnosis of wound infections: Current culturing practices of U.S. Wound care professionals,” *Wounds*, vol. 14, no. 9, pp. 314–328, 2002.

[8] R. Sheybani and A. Shukla, “Highly sensitive label-free dual sensor array for rapid detection of wound bacteria,” *Biosens. Bioelectron.*, 2017.

[9] P. Mostafalu *et al.*, “Smart Bandage for Monitoring and Treatment of Chronic Wounds,” *Small*, vol. 14, no. 33, pp. 1–9, 2018.

[10] B. Mirani *et al.*, “An Advanced Multifunctional Hydrogel-Based Dressing for

Wound Monitoring and Drug Delivery," *Adv. Healthc. Mater.*, vol. 6, no. 19, p. 1700718, Oct. 2017.

[11] L. A. Schneider, A. Korber, S. Grabbe, and J. Dissemond, "Influence of pH on wound-healing: a new perspective for wound-therapy?," *Arch. Dermatol. Res.*, vol. 298, no. 9, pp. 413–420, Jan. 2007.

[12] V. K. Shukla, D. Shukla, S. K. Tiwary, S. Agrawal, and a Rastogi, "Evaluation of pH measurement as a method of wound assessment.," *J. Wound Care*, vol. 16, no. 7, pp. 291–294, 2007.

[13] "How Does Temperature Affect pH? Westlab." [Online]. Available: https://www.westlab.com/blog/2017/11/15/how-does-temperature-affect-ph. [Accessed: 21-Oct-2019].

[14] V. Dini, P. Salvo, A. Janowska, F. Di Francesco, A. Barbini, and M. Romanelli, "Correlation Between Wound Temperature Obtained With an Infrared Camera and Clinical Wound Bed Score in Venous Leg Ulcers.," *Wounds a Compend. Clin. Res. Pract.*, vol. 27, no. 10, pp. 274–8, Oct. 2015.

[15] M. Desrosiers, Z. Bendouah, and J. Barbeau, "Effectiveness of topical antibiotics on Staphylococcus aureus biofilm in vitro.," *Am. J. Rhinol.*, vol. 21, no. 2, pp. 149–53.

[16] T. R. Dargaville, B. L. Farrugia, J. A. Broadbent, S. Pace, Z. Upton, and N. H. Voelcker, "Sensors and imaging for wound healing: A review," *Biosensors and Bioelectronics*. 2013.

[17] R. Czajka, "Development of medical textile market," *Fibres Text. East. Eur.*, vol. 13, no. 1, pp. 13–15, 2005.

[18] A. Koh *et al.*, “A soft, wearable microfluidic device for the capture, storage, and colorimetric sensing of sweat,” *Sci. Transl. Med.*, vol. 8, no. 366, p. 366ra165, Nov. 2016.

[19] L. Shen, J. A. Hagen, and I. Papautsky, “Point-of-care colorimetric detection with a smartphone,” *Lab Chip*, vol. 12, no. 21, p. 4240, Oct. 2012.

[20] S. Coyle *et al.*, “BIOTEX—Biosensing Textiles for Personalised Healthcare Management,” *IEEE Trans. Inf. Technol. Biomed.*, vol. 14, no. 2, pp. 364–370, Mar. 2010.

[21] V. F. Curto *et al.*, “Real-time sweat pH monitoring based on a wearable chemical barcode micro-fluidic platform incorporating ionic liquids,” *Sensors Actuators B Chem.*, vol. 171–172, pp. 1327–1334, Aug. 2012.

[22] P. Kassal, M. Zubak, G. Scheipl, G. J. Mohr, M. D. Steinberg, and I. Murković Steinberg, “Smart bandage with wireless connectivity for optical monitoring of pH,” *Sensors Actuators B Chem.*, vol. 246, pp. 455–460, Jul. 2017.

[23] P. Kassal *et al.*, “Smart bandage with wireless connectivity for uric acid biosensing as an indicator of wound status,” *Electrochem. commun.*, vol. 56, pp. 6–10, Jul. 2015.

[24] P. Mostafalu, W. Lenk, M. R. Dokmeci, B. Ziaie, A. Khademhosseini, and S. R. Sonkusale, “Wireless Flexible Smart Bandage for Continuous Monitoring of Wound Oxygenation,” *IEEE Trans. Biomed. Circuits Syst.*, vol. 9, no. 5, pp. 670–677, Oct. 2015.

[25] M. Punjiya, H. R. Nejad, P. Mostafalu, and S. Sonkusale, “pH sensing threads with

CMOS readout for Smart Bandages," in *2017 IEEE International Symposium on Circuits and Systems (ISCAS)*, 2017, pp. 1–4.

[26] P. Mostafalu *et al.*, "A Textile Dressing for Temporal and Dosage Controlled Drug Delivery," *Adv. Funct. Mater.*, vol. 27, no. 41, p. 1702399, Nov. 2017.

[27] P. Mostafalu, M. Akbari, K. A. Alberti, Q. Xu, A. Khademhosseini, and S. R. Sonkusale, "A toolkit of thread-based microfluidics, sensors, and electronics for 3D tissue embedding for medical diagnostics," *Microsystems Nanoeng.*, vol. 2, no. March, 2016.

[28] K. H. Leong, S. Ramakrishna, Z. M. Huang, and G. A. Bibo, "Potential of knitting for engineering composites - a review," *Compos. Part A Appl. Sci. Manuf.*, vol. 31, no. 3, pp. 197–220, 2000.

[29] M. Stoppa and A. Chiolerio, "Wearable electronics and smart textiles: A critical review," *Sensors (Switzerland)*, vol. 14, no. 7, pp. 11957–11992, 2014.

[30] T. Lindfors and A. Ivaska, "pH sensitivity of polyaniline and its substituted derivatives," *J. Electroanal. Chem.*, vol. 531, no. 1, pp. 43–52, 2002.

[31] A. von Meier, *Electric Power Systems: A Conceptual Introduction - Alexandra von Meier - Google Books*. 2006.

[32] A. S. Nastase, "How to Derive the RMS Value of Pulse and Square Waveforms." [Online]. Available: https://masteringelectronicsdesign.com/how-to-derive-the-rms-value-of-pulse-and-square-waveforms/.

[33] X. Z. Zhang and R. X. Zhuo, "Dynamic properties of temperature-sensitive poly(N-isopropylacrylamide) gel cross-linked through siloxane linkage," *Langmuir*, vol. 17,

no. 1, pp. 12–16, 2001.

[34] S. Bagherifard *et al.*, “Dermal Patch with Integrated Flexible Heater for on Demand Drug Delivery,” *Adv. Healthc. Mater.*, vol. 5, no. 1, pp. 175–184, 2016.

[35] Q. Xu *et al.*, “Preparation of monodisperse biodegradable polymer microparticles using a microfluidic flow-focusing device for controlled drug delivery,” *Small*, vol. 5, no. 13, pp. 1575–1581, Jul. 2009.

[36] R. Hosseinzadeh *et al.*, “A Drug-Eluting 3D-Printed Mesh (GlioMesh) for Management of Glioblastoma,” *Adv. Ther.*, p. 1900113, Oct. 2019.

[37] “Compound Summary Ciprofloxacin,” *U.S. National Library of Medicine*. [Online]. Available: https://pubchem.ncbi.nlm.nih.gov/compound/Ciprofloxacin.

[38] Hardy diagnostics, “MCFARLAND LATEX STANDARDS - IFU Instructions for use.” [Online]. Available: https://catalog.hardydiagnostics.com/cp_prod/Content/hugo/McFarlandStds.htm. [Accessed: 17-Oct-2019].

[39] M. S. Hu *et al.*, “An Improved Humanized Mouse Model for Excisional Wound Healing Using Double Transgenic Mice,” *Adv. Wound Care*, vol. 7, no. 1, pp. 11–17, Jan. 2018.

[40] K. Takao and T. Miyakawa, “Genomic responses in mouse models greatly mimic human inflammatory diseases.,” *Proc. Natl. Acad. Sci. U. S. A.*, vol. 112, no. 4, pp. 1167–72, Jan. 2015.

[41] M. J. Justice and P. Dhillon, “Using the mouse to model human disease: Increasing validity and reproducibility,” *DMM Dis. Model. Mech.*, vol. 9, no. 2, pp. 101–103,

Feb. 2016.

[42] E. E. Friedrich and N. R. Washburn, “Transport patterns of anti-TNF-α in burn wounds: Therapeutic implications of hyaluronic acid conjugation,” *Biomaterials*, vol. 114, pp. 10–22, Jan. 2017.

[43] X. LIU *et al.*, “Direct comparison of the potency of human mesenchymal stem cells derived from amnion tissue, bone marrow and adipose tissue at inducing dermal fibroblast responses to cutaneous wounds,” *Int. J. Mol. Med.*, vol. 31, no. 2, pp. 407–415, Feb. 2013.

[44] D. C. Roy *et al.*, “Ciprofloxacin-loaded keratin hydrogels reduce infection and support healing in a porcine partial-thickness thermal burn,” *Wound Repair Regen.*, vol. 24, no. 4, pp. 657–668, 2016.

[45] R. Sripriya, M. S. Kumar, M. R. Ahmed, and P. K. Sehgal, “Collagen bilayer dressing with ciprofloxacin, an effective system for infected wound healing,” *J. Biomater. Sci. Polym. Ed.*, vol. 18, no. 3, pp. 335–351, 2007.

[46] C. Li *et al.*, “Silver nanoparticles/chitosan oligosaccharide/poly(vinyl alcohol) nanofiber promotes wound healing by activating TGFβ1/Smad signaling pathway.,” *Int. J. Nanomedicine*, vol. 11, pp. 373–86, 2016.